Received: 26 August 2021 | Accepted: 7 October 2021

DOI: 10.1111/ene.15140

european journal of neurology
the official journal of the european academy of neurology

ORIGINAL ARTICLE

Immune profile and radiological characteristics of progressive multifocal leukoencephalopathy

Pia S. Zeiner[1,2,3,4,5] | Leonhard Mann[2,6,7] | Katharina Filipski[3,4,5,6] | Tatjana Starzetz[6] | Marie-Therese Forster[8] | Michael W. Ronellenfitsch[1,3,4,5] | Joachim P. Steinbach[1,3,4,5] | Michel Mittelbronn[9,10,11,12,13,14] | Marlies Wagner[3,4,5,7] | Patrick N. Harter[3,4,5,6]

[1]Dr Senckenberg Institute of Neurooncology, University Hospital, Frankfurt am Main, Germany

[2]Department of Neurology, University Hospital, Frankfurt am Main, Germany

[3]Frankfurt Cancer Institute (FCI), Frankfurt am Main, Germany

[4]German Cancer Consortium (DKTK), Heidelberg, Germany

[5]German Cancer Research Center (DKFZ), Heidelberg, Germany

[6]Neurological Institute (Edinger Institute), University Hospital, Frankfurt am Main, Germany

[7]Institute of Neuroradiology, Goethe University, Frankfurt am Main, Germany

[8]Department of Neurosurgery, Goethe University, Frankfurt am Main, Germany

[9]Luxembourg Centre for Systems Biomedicine (LCSB), University of Luxembourg, Esch-sur-Alzette, Luxembourg

[10]Department of Oncology (DONC), Luxembourg Institute of Health (LIH), Strassen, Luxembourg

[11]Faculty of Science, Technology and Medicine (FSTM), University of Luxembourg, Esch-sur-Alzette, Luxembourg

[12]Department of Life Sciences and Medicine (DLSM), University of Luxembourg, Esch-sur-Alzette, Luxembourg

[13]Laboratoire national de santé (LNS), Dudelange, Luxembourg

[14]Luxembourg Centre of Neuropathology (LCNP), University of Luxembourg, Esch-sur-Alzette, Luxembourg

Correspondence
Pia S. Zeiner, Dr Senckenberg Institute of Neurooncology, University Hospital, Heinrich-Hoffmann Str. 7, 60528 Frankfurt, Germany.
Email: pia.zeiner@kgu.de

Funding information
JPS and MWR received funding by the State of Hessen (LOEWE). PSZ and KF received intramural 'Frankfurt Research Funding'. The Dr. Senckenberg Institute of Neurooncology is supported by the Dr. Senckenberg Foundation. MWR received a grant from UCB. MM is supported by the Luxembourg National Research Fond (PEARL P16/BM/11192868 grant). PSZ and KF received funding by the Mildred-Scheel Foundation.

Abstract

Background and purpose: Progressive multifocal leukoencephalopathy (PML) constitutes a severe disease with increasing incidence, mostly in the context of immunosuppressive therapies. A detailed understanding of immune response in PML appears critical for the treatment strategy. The aim was a comprehensive immunoprofiling and radiological characterization of magnetic resonance imaging (MRI) defined PML variants.

Methods: All biopsy-confirmed PML patients ($n = 15$) treated in our department between January 2004 and July 2019 were retrospectively analysed. Data from MRI, histology as well as detailed clinical and outcome data were collected. The MRI-defined variants of classical (cPML) and inflammatory (iPML) PML were discriminated based on the intensity of gadolinium enhancement. In these PML variants, intensity and localization (perivascular vs. parenchymal) of inflammation in MRI and histology as well as the cellular composition by immunohistochemistry were assessed. The size of the demyelinating lesions was correlated with immune cell infiltration.

Results: Patients with MRI-defined iPML showed a stronger intensity of inflammation with an increased lymphocyte infiltration on histological level. Also, iPML was characterized by a predominantly perivascular inflammation. However, cPML patients also

See commentary by D. B. Clifford on page 373

demonstrated certain inflammatory tissue alterations. Infiltration of CD163-positive microglia and macrophage (M/M) subtypes correlated with PML lesion size.

Conclusions: The non-invasive MRI-based discrimination of PML variants allows for an estimation of inflammatory tissue alterations, although exhibiting limitations in MRI-defined cPML. The association of a distinct phagocytic M/M subtype with the extent of demyelination might reflect disease progression.

KEYWORDS
biomarker, immune response, MRI, neuroimaging, PML

INTRODUCTION

Progressive multifocal leukoencephalopathy (PML) is a demyelinating disease of the central nervous system (CNS) caused by a reactivation of the JC virus (JCV) belonging to the polyoma group [1,2]. PML constitutes one of the most dismal neurological disorders usually occurring in acquired or hereditary immunocompromised conditions such as human immunodeficiency virus (HIV) infection, neoplasia or treatments for different autoimmune diseases [3]. Lately, the incidence of PML is increasing as a result of a variety of efficient next generation immunosuppressive treatments like monoclonal antibodies in patients with autoimmune diseases [4]. Unusual cases of PML without apparent immunosuppression are reported [5,6].

In patients with HIV-related PML, demyelination is the most prominent characteristic in magnetic resonance imaging (MRI), barely showing any signs of inflammation (so-called 'classical PML' [cPML]). In contrast, approximately 30% of patients with monoclonal-antibody-related PML show inflammatory contrast-enhancing lesions in MRI recently coining the umbrella term 'inflammatory PML' (iPML) [7]. In some of these patients, punctuate T2 lesions and punctuate contrast enhancement were described as a potential surrogate for perivascular localization of inflammation [8,9]. Additionally, contrast enhancement is described as the leading imaging finding in PML patients with inflammatory signs [10]. A precise conceptual delimitation of the terms iPML and PML-immune reconstitution inflammatory syndrome (IRIS) is lacking [11]. Both are allocated to similar imaging and histopathological features and therefore most probably constitute the same pathophysiological condition. PML-IRIS is described as associated with paradoxical clinical deterioration, high morbidity and mortality triggered by forced immune reconstitution [3,12]. IRIS is not specific for PML but may also occur in other opportunistic infectious diseases [13].

For PML treatment virostatic therapies have been proposed without resounding success [14,15]. Thus, therapeutic strategies aim to re-establish CNS immune surveillance via combined antiretroviral therapy in HIV-related PML [16] or cessation and clearance of trigger substances [12]. Promising results were shown for a treatment approach based on immune checkpoint inhibitors that augment immune response [17]. In contrast, therapeutic management of the inflammatory PML variants is based on steroid treatment and newer anti-inflammatory agents are being tested [18].

Because of the lack of targeted treatments for PML, prevention and early recognition by risk stratification and improved diagnostic tools are crucial [2]. Diagnosis of PML is based on clinical and neuroradiological findings as well as the detection of JCV DNA in the cerebrospinal fluid (CSF), which can be difficult in patients with a relatively intact immune system and low JCV copy numbers [19,20]. In these patients, stereotactic brain biopsy is applied for JCV detection [21]. The histopathological hallmarks of PML lesions—comprising a demyelination alongside JCV-infected oligodendrocytes with nuclear inclusions and a reactive gliosis with bizarre astrocytes—are well established [3,19]. However, the underlying mechanisms of innate and adaptive immune responses controlling JCV infection are poorly understood. Although microglia and macrophages (M/M) account for the majority of immune cells in PML lesions [22,23], there are hardly any studies systematically profiling an innate immune response. Data about a potential association of immune infiltration with clinical parameters or neuroradiological PML characteristics [19,22] are sparse and controversial due to small patient cohorts. MRI was so far rather applied to exclude PML than to frame the diagnosis [19,24]. A comprehensive characterization of infiltrating immune cell subsets in PML lesions and its correlation with radiological PML variants is much needed given the therapeutic relevance of the inflammatory status of the PML that implicates a decision for an immune enhancing or inhibitory treatment concept.

The immune cell landscape and radiological characteristics were retrospectively characterized in all patients diagnosed with PML at our department over a 15-year period.

MATERIALS AND METHODS

Study design and data collection

This retrospective study included all patients diagnosed with definite PML according to the American Academy of Neurology consensus statement [19] who underwent brain biopsy with detection of JCV in brain tissue in our department from January 2004 to July 2019 (Figure 1a, Tables S1 and S2). The MRI-defined terms iPML and cPML based on the intensity of gadolinium enhancement (see below) were applied. Additionally, a cohort of eight non-PML control patients (Table S3) with inflammatory CNS pathologies

of different aetiologies was used for immunohistochemical (IHC) analyses. JCV in brain tissue was negative in all non-PML control patients. The following additional parameters were included for each case: epidemiological characteristics such as sex and age at PML diagnosis, Karnofsky Performance Status at PML diagnosis, underlying disease, duration of underlying disease and respective treatment with regard to PML diagnosis, diagnostic latency (in months) between symptom onset and brain biopsy, CD4 lymphocytopenia, JCV detection in CSF, CSF pleocytosis (>4 cells/μl), PML treatment approach and clinical outcome (overall survival from bioptic PML diagnosis).

In situ hybridization for JCV detection

Manual in situ hybridization (ISH) for JCV detection and consecutive diagnosis of PML was applied. Paraffin-embedded tissue specimens were deparaffinized and rehydrated, followed by blocking of endogenous peroxidase with H_2O_2 solution (15 min at room temperature) and proteinase K pre-treatment (15 min at 37°C). In situ hybridization was performed overnight at 37°C with a hybridization mix containing 50% deionized formamide, 10% dextrane sulfate, 2× SSPE buffer and 1 μg/ml of the biotinylated JCV DNA probe (JC Virus BioProbe, Enzo Life Sciences, Lörrach, Germany), followed by treatment with saline-sodium citrate (SSC) buffer (2× SCC 1 h at 37°C, 1× SCC 1 h at 37°C, two times 0.5× SCC for 30 min at 37°C). Detection was performed by direct affinity cytochemistry utilizing a streptavidin-biotin-peroxidase complex.

Histology

Paraffin tissue blocks were cut in 3–4-μm thick slices using a microtome (Leica Microsystems) and mounted on SuperFrost slides (Thermo Scientific). Haematoxylin and eosin (H&E) stainings of paraffin-embedded tissue samples of 15 PML patients were analysed regarding their inflammation pattern (perivascular vs. parenchymal vs. combined perivascular/parenchymal), grade of inflammation intensity (1, weak; 2, moderate, 3, strong), necroses and demyelination (dichotomized yes/no). All specimens were obtained from the tissue archives of the Edinger Institute (Neurological Institute), Frankfurt, Germany. The use of patient material and data was approved by the local ethics committee (432/17). Histological diagnoses of PML patients and a cohort of non-PML control patients were performed by board certified neuropathologists (PNH, MM).

Magnetic resonance imaging analysis

MRI data of 12 corresponding PML patients were available (Figure 1a, Table S2). Follow-up MRI data of four of these patients were available (Table S2). The protocol included T2-weighted images (WI), fluid-attenuated inversion recovery (FLAIR)-WI, T1-WI with and without intravenous contrast application, and diffusion-weighted images (DWI) with apparent diffusion coefficient (ADC) maps. Also, contrast-enhancing and non-enhancing lesions were assessed on all sequences by two neuroradiological readers (LM, MW).

First, the intensity of MRI inflammation (none, poor, moderate or strong) was assessed on contrast enhanced T1-WI. The MRI-defined PML variants of cPML versus iPML were discriminated by the intensity of gadolinium enhancement (cPML, absent, weak; iPML, moderate, strong) resulting in $n = 5$ patients matching the criteria for iPML (Table S1).

Next, the MRI inflammation pattern (perivascular vs. parenchymal vs. mixed perivascular and parenchymal) was evaluated on contrast enhanced T1-WI and T2-WI based on the respective patterns of contrast enhancement and T2 hyperintensity of the lesions.

Demyelination was defined as a flat T2 hyperintense subcortical lesion without mass effect [25]. The intensity of demyelination (weak, moderate, strong) was estimated depending on additional alteration patterns in T1-WI, DWI and ADC maps. Weak demyelination in PML lesions was defined as an only T2 hyperintense signal. Moderate demyelination in PML lesions was defined as an additional T1 hypointense signal as known from multiple sclerosis lesions [26]. Lesions of PML patients with an additional central low DWI signal and peripheral high DWI signal with correspondingly reduced ADC were defined as strong demyelinating lesions [27,28]. The area/size of a demyelinating lesion was measured in FLAIR-WI.

To describe the presence of necrosis, T2- and FLAIR-WI as well as contrast enhanced T1-WI were analysed.

Immunohistochemistry

For IHC the following antibodies were used: anti-CD4 (Roche #790-4423, clone SP35, undiluted), anti-CD8 (Dako, clone C8/144B, dilution for IHC 1:100), anti-CD20 (Dako, clone L20, dilution for IHC 1:500), anti-CD68 (Dako, clone M0876, dilution for IHC 1:200), anti-CD74 (Abcam, ab9514, dilution for IHC 1:100), anti-CD138 (Dako, clone MI15, dilution for IHC 1:200), anti-CD163 (Leica Biosystems, NCL-CD163, dilution for IHC 1:50), anti-CD206 (Abcam, ab117644, dilution for IHC 1:100), anti-Granzyme-B (GrB) (Abcam, ab11198, clone GB7), anti-Iba1 (Wako, 019-19741, dilution for IHC 1:1000) and anti-major histocompatibility complex class II (MHC-II) (Dako, clone M0775, dilution for IHC 1:1000). IHC was performed using standardized automated immunohistochemistry [29].

Manual quantification of immunohistochemistry

Immunohistochemical quantification of different leukocyte markers ($CD4^{high}$- and CD8-positive T lymphocytes, GrB-positive cytotoxic T- and NK-cells, CD20-positive B-cells, Iba1-, $CD4^{low}$-, CD68-, CD74-, CD163-, CD206- and MHC-II-positive M/M and CD138-positive plasma cells) was performed by estimation of the percentage of

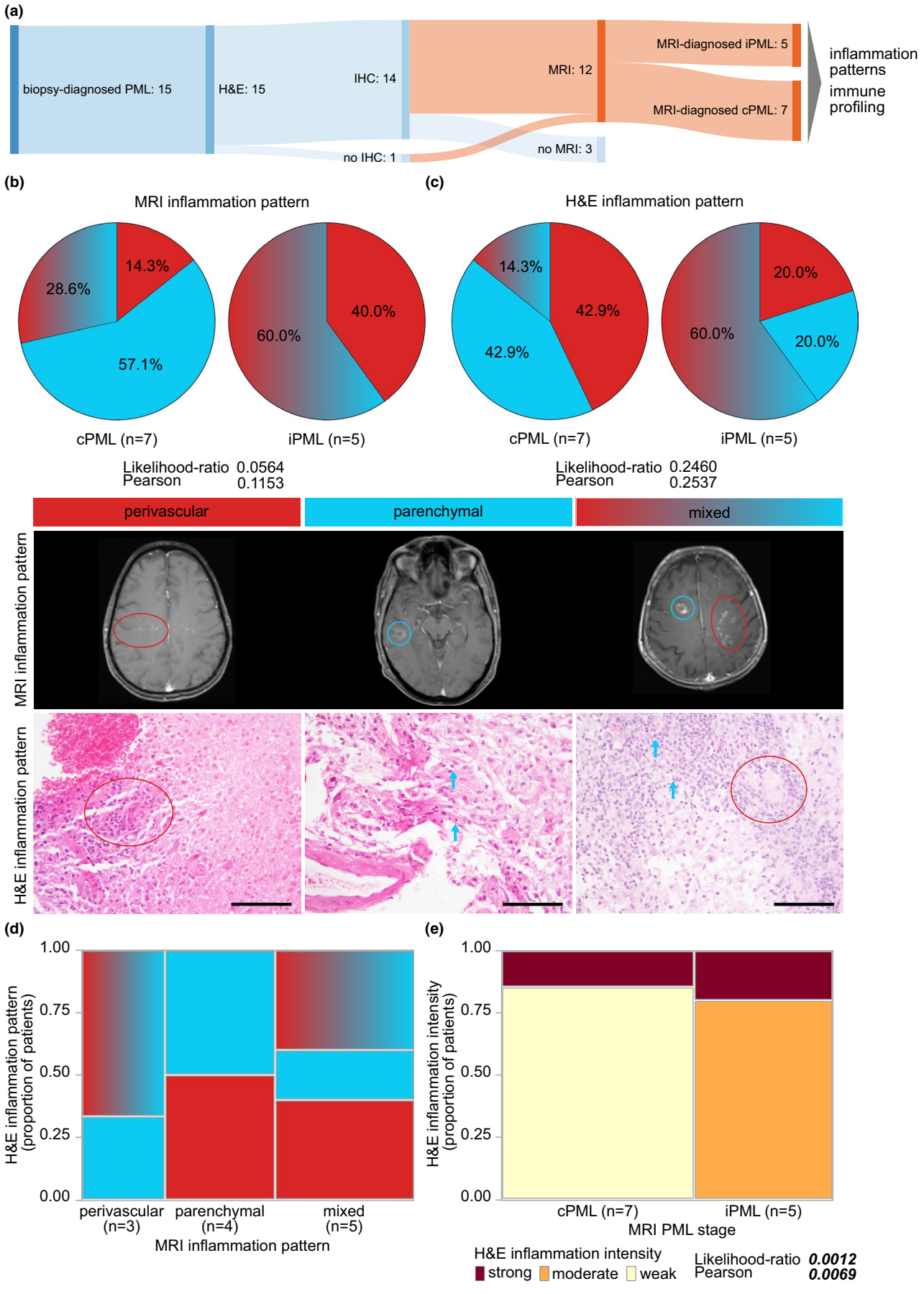

FIGURE 1 Patients with MRI-defined inflammatory PML showed stronger histological inflammation and a perivascular dominated inflammation pattern. (a) The Sankey diagram was created using the SankeyMATIC diagram builder to illustrate the workflow for patients' inclusion. Patients with iPML were differentiated from patients with cPML based on the intensity of gadolinium enhancement in MRI. Pie diagrams showing a dominating perivascular (b) MRI and (c) histological H&E inflammation pattern in iPML patients in contrast to cPML patients (red, perivascular; blue, parenchymal; red/blue, mixed perivascular and parenchymal inflammation pattern). (b), (c) (lower panel) Representative MRI images of PML patients showing a distinct pattern of inflammation in contrast enhanced T1-WI reflecting perivascular (red ellipse), parenchymal (blue ellipse) or mixed perivascular and parenchymal inflammation patterns are depicted. MRI inflammation patterns were evaluated on the basis of T2 lesions and contrast enhancement pattern in T1-WI. Representative H&E stainings of PML patients with perivascular (red ellipse), parenchymal (blue arrows) or mixed perivascular and parenchymal inflammation pattern (original magnification 20×, scale bars 100 μm) are depicted. (d) Fractions of patients with perivascular, parenchymal or mixed histological inflammation in the patient groups with perivascular, parenchymal or mixed MRI inflammation. (e) Fractions of patients with weak (yellow), moderate (orange) or strong (red) histological inflammation in MRI-defined cPML versus iPML patients (significant p values ≤0.05 in bold italic) [Colour figure can be viewed at wileyonlinelibrary.com]

positive cells related to the total cell number (PSZ, LM, PNH) of the entire tissue specimen. As for CD4-staining, positive lymphocytes were discriminated from CD4-positive M/M according to morphology and staining intensity ($CD4^{high}$ vs. $CD4^{low}$, evaluated by board certified neuropathologists MM, PNH). Stainings were analysed using a light microscope (BX41, Olympus).

Statistical analyses

Magnetic resonance imaging characteristics of PML patients (see above: perivascular and/or parenchymal inflammation pattern, intensity of gadolinium enhancement, demyelination intensity, size of demyelinating PML lesion) were compared to H&E stainings (see above: perivascular and/or parenchymal inflammation, inflammation intensity, necrosis, demyelination) as well as the infiltration levels of different leukocytes assessed with IHC. Since homoscedasticity and normal distribution were not given for all marker analyses, a nonparametric Wilcoxon test with subsequent adjustment of the p values by the Bonferroni–Holm method was used. Correlation analyses were performed based on Pearson's r and Spearman's ρ testing. Kaplan–Meier survival curves were compared by log-rank and Wilcoxon test for comparison of the overall survival between two groups. Significant p values are indicated ($^*p < 0.05$). Statistical analysis was performed using JMP 15.0 software (SAS). Graphics were prepared using the GraphPad Prism 8 software (GraphPad Software Inc.). The Sankey diagram was created using the SankeyMATIC diagram builder (Figure 1a).

RESULTS

Characteristics of the patient cohort

Fifteen PML patients were identified ($n = 8$ with HIV-related PML; $n = 7$ non-HIV PML patients with other underlying diseases and treatments; see Figure 1a and detailed clinical information in Table S1). None of our non-HIV PML patients was treated with the monoclonal antibody natalizumab that was described to be associated with the iPML MRI pattern [7].

Patients with MRI-defined inflammatory PML showed stronger histological inflammation and a perivascular dominated inflammation pattern

Patients with an MRI-based definition of iPML tend towards a perivascular dominated inflammation pattern both in MRI (pattern of contrast enhancement and T2 lesions evaluated) and histology with a perivascular or mixed (perivascular and parenchymal) inflammation pattern (Figure 1b), whereas MRI-defined cPML patients show a preponderant parenchymal inflammation pattern on MRI and histology (Figure 1c). MRI inflammation patterns (perivascular vs. parenchymal vs. mixed) were not entirely congruent with histology patterns (Figure 1d) nor did they correlate with particular immune cell subsets (Figures S1 and S2). Histological inflammation intensity was significantly stronger in patients with MRI-defined iPML than cPML, although it should be noted that cPML patients also displayed a certain level of inflammatory tissue alterations (Figure 1e).

Patients with iPML showed an increased infiltration of CD8-positive T-cells and CD138-positive plasma cells

Next, the adaptive and innate immune cell infiltration was compared in patients with MRI-defined iPML versus cPML. Lesions of iPML patients showed a significantly higher infiltration of the lymphocytic cell cluster and specifically of CD8-positive T-cells and CD138-positive plasma cells compared to cPML lesions (Figure 2a–c). The myeloid cell cluster and all other investigated immune cell subsets did not show statistically significant differences between iPML and cPML (Figures 2d,e, S3 and S4). Patients with cPML and iPML did not show a significant difference in overall survival (Figure 2f).

Infiltration with microglia and macrophages was a general hallmark of PML lesions

Generally, immune infiltrates of PML lesions predominantly comprised M/M besides different effector immune cells (Figure 3). Patients suffering from different inflammatory CNS pathologies without JCV detection in biopsy (Table S3) were included as a

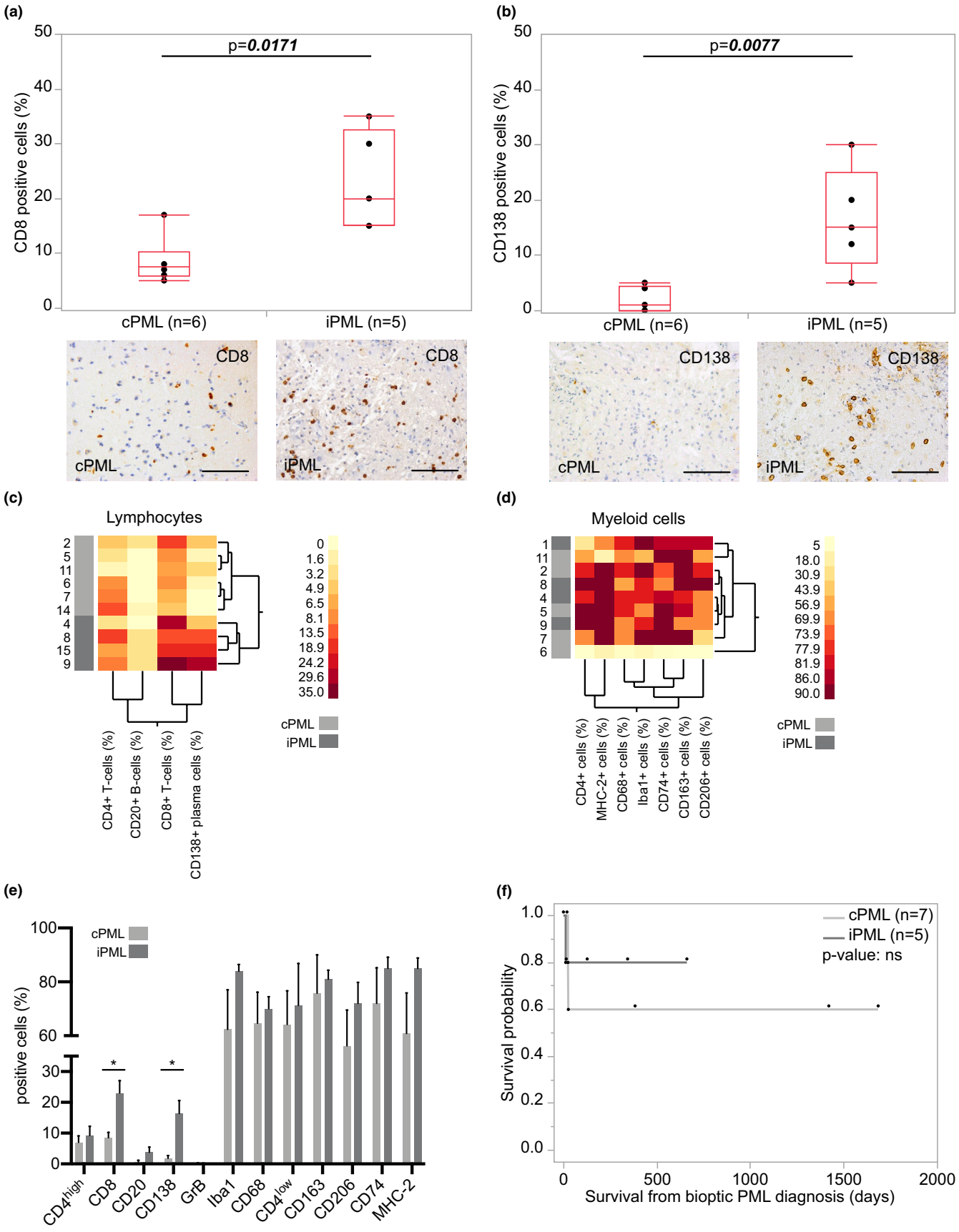

FIGURE 2 CD8-positive T-cells and CD138-positive plasma cells were increased in lesions of inflammatory PML patients. (a), (b) Box and whisker plots for significant comparisons of infiltration levels (%) with (a) CD8-positive and (b) CD138-positive cells (%) in iPML and cPML patients as well as representative immunohistochemistry stainings (original magnification 20×, scale bars 100 μm; significant *p* values ≤0.05 depicted in bold italic). (c), (d) Heatmap of the patient samples (rows, PML variant defined by MRI depicted) showing the proportions of (c) lymphocytes and (d) myeloid cells (d). Unsupervised hierarchical clustering revealed two distinct clusters in cPML (light grey) and iPML (dark grey) patients. (e) Percentages of immune cells were compared in lesions of cPML (light grey) and iPML (dark grey) patients (SEM error bars are depicted and significant comparisons in Wilcoxon testing ≤0.05 are indicated with an asterisk). (f) Kaplan–Meier survival curves separating cPML (light grey) from iPML (dark grey) patients. Overall survival from PML diagnosis was compared by log-rank and Wilcoxon test (*p* values not significant, ns) [Colour figure can be viewed at wileyonlinelibrary.com]

non-PML control cohort for IHC analyses. In comparison to these non-PML patients, the M/M subsets expressing CD74 (functionally involved in antigen presentation) and CD163 (functionally involved in phagocytosis) as well as CD8-positive T-cells were found in considerably higher amounts in PML lesions (Figure 3).

Infiltration of CD163-positive microglia and macrophages correlated with PML lesion size

Next, the extent of demyelination in MRI as a key PML feature was correlated with the immune cell infiltration as assessed by IHC. A significant correlation of the MRI-assessed size of demyelinating PML lesions with the infiltration of CD163-positive M/M was found (Figure 4a). A similar trend (yet missing statistical significance as for example for the CD206-positive M/M subtype) could be observed for all investigated M/M subpopulations (Figure S5), in contrast to effector immune cell infiltration (Figure S6). Patients with an above- or below-median size of the demyelinating PML lesion did not show a significant difference in overall survival (Figure 4b). In contrast to the actual size of MRI demyelination, the intensity of MRI demyelination showed no significant correlation with a particular immune cell subset (Figures 4c, S7 and S8).

Against the background that particular histological parameters (CD163-positive M/M infiltration) may be a surrogate for disease progression, our interest was in the temporal dynamics of our radiological features. Follow-up MRI showed a decrease of the demyelinating lesion sizes in two patients with clinical improvement and longer-term follow-up periods (patients 2 and 6), whilst the actual MRI-defined PML variants remained stable in long- and short-term follow-up MRI. The MRI inflammation pattern (parenchymal, perivascular, mixed) did change in one of the four patients (patient 6) who lost the perivascular inflammation component in a time period of 1493 days between the two MRIs (Figure 5, Table S2) when he also received steroid treatment (Table S1).

DISCUSSION

PML constitutes a severe clinical condition in immunosuppressed patients. Diagnostic, preventive and targeted therapeutic standards based on prospective clinical trials are hard to establish due to its low incidence, diverse triggers and highly individual disease dynamics. The incidence of PML is increasing due to the rising application of certain immunosuppressive and immunomodulatory drugs [4] such as monoclonal antibodies for treatment of multiple sclerosis [7,10]. The still remarkable diagnostic uncertainty, often reflected by a substantial latency until diagnosis confirmation (as also apparent in our cohort; Table S1), originates from a lack of pathognomonic clinical and neuroradiological features as well as a considerable high rate of false-negative results in CSF testing. Robust clinical, radiological or histological biomarkers of predictive or prognostic value that also consider the different MRI-defined PML variants, that may constitute a continuous spectrum, are lacking. Also, a better understanding of adaptive and innate immune response in iPML and cPML patients including a characterization on a cellular level appears critical. So far, small-scale attempts [24] of historadiological correlation lack a detailed analysis of different immune cell types [22]. However, several smaller studies stress the importance of a cellular characterization of PML lesions for the understanding of pathogenesis and the identification of prognostic biomarkers [23,24,30–32].

Therefore, the aim was to perform a broad histological-radiological characterization of PML patients with the different MRI-defined variants cPML and iPML that were differentiated based on the intensity of gadolinium enhancement in MRI. Interestingly, a perivascular dominated inflammation pattern both in MRI (evaluation of contrast enhancement as well as T2 lesions) and histology turned out to be a hallmark of our iPML in contrast to cPML patients who displayed a rather parenchymal inflammation pattern (Figure 1b). Of note, the absence of gadolinium enhancement as a nonspecific sign of blood–brain barrier impairment [10,24] does not exclude inflammatory PML alterations [24,33,34]. In line with this, cPML patients of our cohort likewise displayed inflammatory alterations in histology (Figure 1c,d), although histological inflammation intensity was significantly stronger in patients with iPML (Figure 1e). More specifically, IHC-based cellular classification revealed higher amounts of CD8-positive T-cells and CD138-positive plasma cells in iPML than cPML patients (Figure 2). This supports the hypothesis of a pathophysiological role of plasma cells in this context [3,24,32] that even correlate with an intrathecal antibody synthesis against JCV viral protein 1 [35]. Similarly, CD8-positive T-cells were suggested as a biomarker in some studies [24,30] with a potentially negative prognostic role in PML-IRIS [30,31] that could not be observed in our cohort with respect to overall survival (data not shown). The detailed underlying pathophysiological mechanisms of these findings are still unclear [3,36,37]. Other leukocyte subsets such as CD4-positive lymphocytes might also play a role in iPML [23]. Taken together, MRI-based stratification of cPML and iPML allows for an estimation

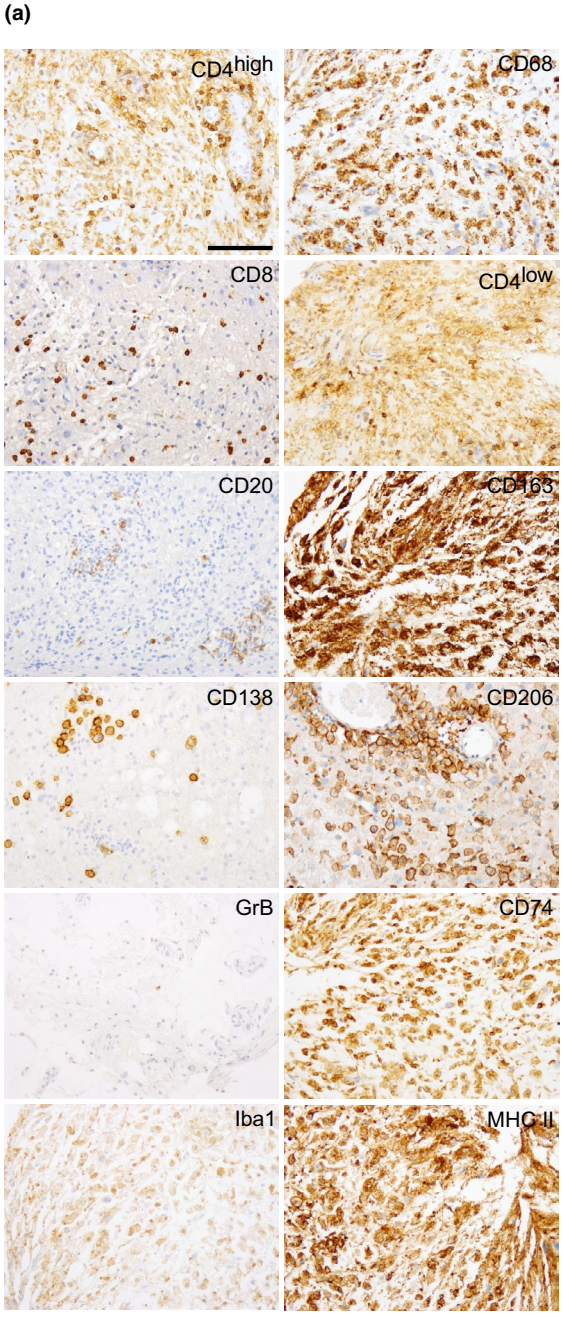

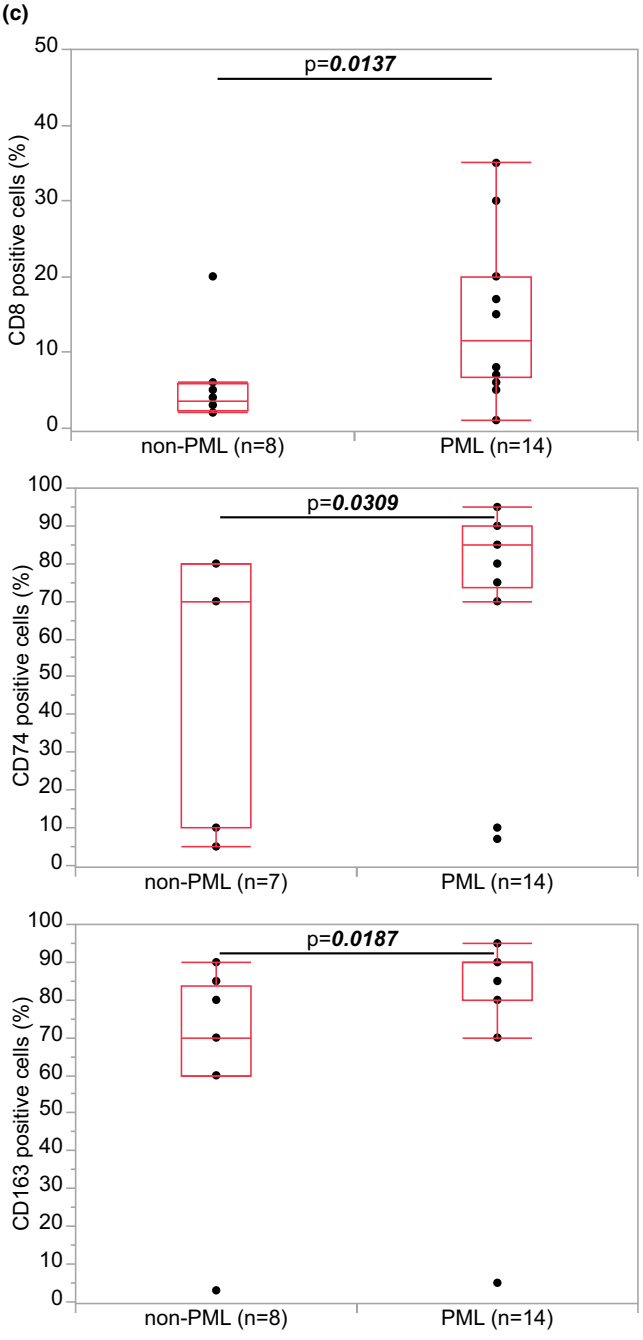

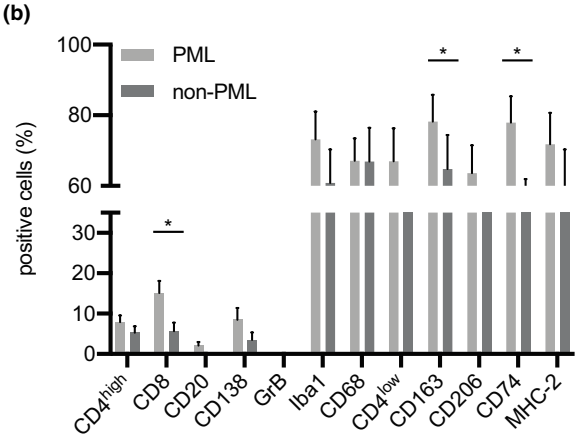

FIGURE 3 PML lesions were dominated by microglia/macrophage infiltration. (a) Representative immunohistochemical stainings for infiltrating immune cell subsets in PML lesions are depicted for $CD4^{high}$- and CD8-positive T-cells, GrB-positive cytotoxic T- and NK-cells, CD20-positive B-cells, CD138-positive plasma cells, Iba1-, $CD4^{low}$-, CD68-, CD74-, CD163-, CD206- and MHC-II-positive microglia/macrophages (original magnification 20×, scale bars 100 μm). (b) Percentages of immune cells were compared in lesions of PML (light grey) and non-PML (dark grey) patients (SEM error bars are depicted and significant comparisons in Wilcoxon testing ≤0.05 are indicated with an asterisk). (c) Box and whisker plots for significant comparisons of infiltration levels (positive cells, %) with CD8-positive, CD74-positive and CD163-positive cells in PML and non-PML patients are depicted (significant *p* values ≤0.05 in bold italic) [Colour figure can be viewed at wileyonlinelibrary.com]

FIGURE 4 Infiltration with CD163-positive microglia and macrophages correlated with PML lesion size. (a) Correlation analyses revealed a significantly positive association of the infiltration with CD163-positive microglia and macrophages with the size of the demyelinating lesion in PML patients (determined by MRI, mm^2). The table depicts the correlation coefficients r^2 and Spearman's ρ with the respective *p* values of CD163- and CD206-positive microglia/macrophages as well as the PML lesion size (significant *p* values ≤0.05 in italic). (b) Kaplan–Meier survival curves separating patients with below- and above-median PML lesion size. Overall survival from PML diagnosis is compared by log-rank and Wilcoxon test (*p* values not significant, ns). (c) Representative images of a weak, moderate and strong demyelination intensity of PML lesions in MRI FLAIR sequence [Colour figure can be viewed at wileyonlinelibrary.com]

(a)

	CD163-positive cells (%)	CD206-positive cells (%)	Size of PML-lesion (mm^2)
CD163-positive cells (%)		ρ=0.4801, p=0.0823 *r^2=0.5249, p=0.0034*	*ρ=0.6778, p=0.0219* r^2=0.2775, p=0.0960
CD206-positive cells (%)	ρ=0.4801, p=0.0823 *r^2=0.5249, p=0.0034*		ρ=0.5656, p=0.0698 r^2=0.3039, p=0.0787
Size of PML-lesion (mm^2)	*ρ=0.6778, p=0.0219* r^2=0.2775, p=0.0960	ρ=0.5656, p=0.0698 r^2=0.3039, p=0.0787	

(b)

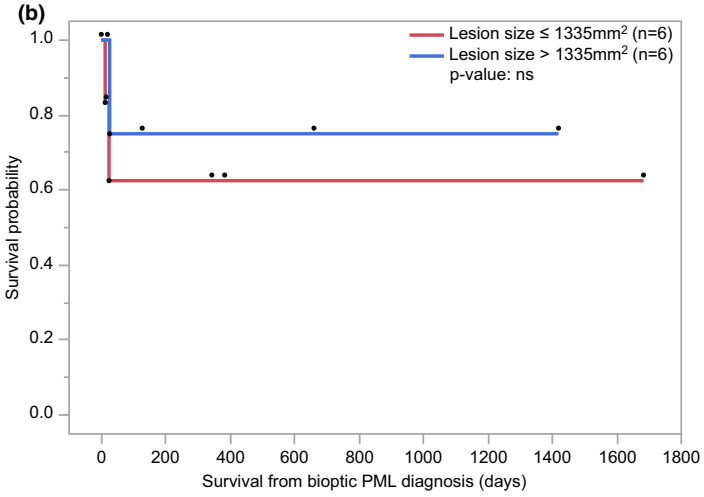

(c)

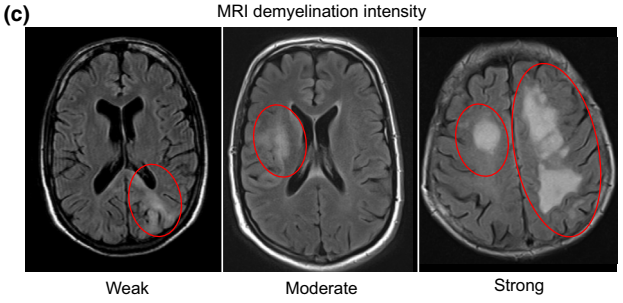

of the extent of inflammation and may therefore serve as a non-invasive and easily accessible tool to identify patients who may benefit from anti-inflammatory treatment. However, it should be stated that this method is a simplification of the actual inflammatory tissue status and has its limitations especially in patients with MRI-defined cPML but marked inflammatory tissue alterations (Figure 1c,e).

As for the comprehensive characterization of immune cell infiltration in PML lesions performed in our study, M/M infiltration was found as a general hallmark of PML lesions (Figure 3), which is in line with studies based on pan-M/M markers without a consideration of different M/M subsets [22,23]. One study suggests CD68-positive M/M as a positive prognostic factor in PML [30]. Another study claims that CD68-positive M/M reflect a particular inflammatory state of PML lesions [38]. However, both studies are limited to low patient numbers and an analysis of only individual cell types. Interestingly, CD163- and CD74-positive M/M subtypes as well as CD8-positive T-cells were found in higher amounts in PML lesions in comparison to lesions of our control cohort of different non-PML inflammatory CNS diseases (Figure 3). As for CD74, this MHC-II chaperone molecule was recently discovered to be an M/M marker in gliomas, where high levels of CD74-positive M/M are associated with prolonged survival and a potentially pro-inflammatory immune microenvironment [29]. Besides its function in antigen presentation, CD74 is known as a surface receptor for the pro-inflammatory cytokine macrophage migration inhibitory factor [39] with pleiotropic pro-inflammatory effects that could play a role in PML pathophysiology. Since the heterogeneity of our control cohort was a clear limitation of our study, further studies including survival analysis and a functional characterization

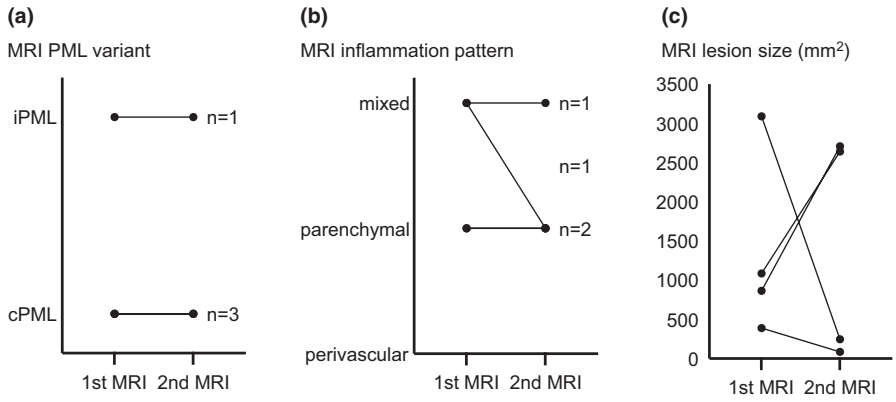

FIGURE 5 MRI follow-up analyses of patients with classical and inflammatory PML. Pairwise comparisons of initial and follow-up MRIs from patients with MRI-defined cPML ($n = 3$) and iPML ($n = 1$) in the first MRI for the parameters (a) PML variant (cPML or iPML), (b) MRI inflammation pattern (perivascular, parenchymal or mixed) and (c) MRI lesion size (mm^2). Detailed characterization of follow-up MRIs is depicted in Table S2 and the corresponding clinical characteristics in Table S1

are needed to investigate whether the findings demonstrated in Figure 3 really reflect a pathognomonic feature or an association with disease development and progression of PML patients. Whilst demyelination is a cardinal feature of PML, a significantly positive correlation of the size of the demyelinating PML lesion with the infiltration of the CD163-positive M/M subtype was additionally found (Figure 4). A similar trend could be observed for all M/M subpopulations (Figure S5). Since the scavenger receptor CD163 is functionally involved in phagocytosis as previously shown in glioma-associated M/M [40], increasing amounts of this M/M subtype might reflect the phagocytic environment of PML lesions. Therefore, the positive correlation of CD163-positive M/M with the increasing size of demyelination might be an expression of disease progression. The MRI-defined PML variants diagnosed in the first imaging remained stable in long- and short-term follow-up. However, these analyses should be regarded as pilot data and interpreted with caution due to the lower patient numbers. Sequential radio-histological investigations within individual patients who were not available in the context of our study would be necessary to validate these findings.

In conclusion, this study provides evidence that the non-invasive investigation of MRI-defined PML variants might help in estimating inflammatory tissue alterations. Additionally, a subset of CD163-positive M/M was associated with the extent of MRI demyelination and therefore potentially with disease progression. In the light of the increasing incidence of PML, future prospective studies in larger patient cohorts are indispensable to confirm these findings and investigate their potential clinical relevance.

ACKNOWLEDGEMENTS

PSZ and KF received intramural 'Frankfurt Research Funding' and by the Mildred-Scheel Foundation. MWR received a grant from UCB. JPS and MWR received funding by the State of Hessen (LOEWE). The Dr Senckenberg Institute of Neurooncology is supported by the Dr Senckenberg Foundation. MM is supported by the Luxembourg National Research Fond (PEARL P16/BM/11192868 grant).

CONFLICT OF INTEREST

There is no conflict of interest regarding the publication of this article.

AUTHOR CONTRIBUTIONS

Conception and design of the work: PSZ, MM, MW, PNH. Acquisition, analysis and interpretation of data: PSZ, LM, KF, TS, MTF, MWR, JPS, MM, MW, PNH. Drafting of the manuscript: PSZ, LM, PNH. Critical revision for important intellectual content: all authors.

ETHICAL APPROVAL

The study was approved by the local ethics committee (432/17). Due to the retrospective character, the ethics committee explicitly allowed a waiver for obtaining written consent of participants.

DATA AVAILABILITY STATEMENT

The data that support the findings of this study are available from the corresponding author upon reasonable request.

ORCID

Pia S. Zeiner https://orcid.org/0000-0001-6626-9211
Michael W. Ronellenfitsch https://orcid.org/0000-0002-1402-6290

REFERENCES

1. Bellizzi A, Anzivino E, Rodio DM, Palamara AT, Nencioni L, Pietropaolo V. New insights on human polyomavirus JC and pathogenesis of progressive multifocal leukoencephalopathy. *Clin Dev Immunol*. 2013;2013:839719. https://doi.org/10.1155/2013/839719
2. Ferenczy MW, Marshall LJ, Nelson CDS, et al. Molecular biology, epidemiology, and pathogenesis of progressive multifocal leukoencephalopathy, the JC virus-induced demyelinating disease of the human brain. *Clin Microbiol Rev*. 2012;25(3):471-506. https://doi.org/10.1128/CMR.05031-11
3. Bauer J, Gold R, Adams O, Lassmann H. Progressive multifocal leukoencephalopathy and immune reconstitution inflammatory syndrome (IRIS). *Acta Neuropathol*. 2015;130(6):751-764. https://doi.org/10.1007/s00401-015-1471-7

4. Schmedt N, Andersohn F, Garbe E. Signals of progressive multifocal leukoencephalopathy for immunosuppressants: a disproportionality analysis of spontaneous reports within the US Adverse Event Reporting System (AERS). *Pharmacoepidemiol Drug Saf*. 2012;21(11):1216-1220. https://doi.org/10.1002/pds.3320
5. Grewal J, Dalal P, Bowman M, Kaya B, Otero JJ, Imitola J. Progressive multifocal leukoencephalopathy in a patient without apparent immunosuppression. *J Neurovirol*. 2016;22(5):683-687. https://doi.org/10.1007/s13365-016-0459-y
6. Vaklavas C, Sotelo-Rafiq EP, Lovy J, Escobar MA, Tsimberidou AM. Progressive multifocal leukoencephalopathy in a patient without apparent immunosuppression. *Virol J*. 2010;7:256. https://doi.org/10.1186/1743-422X-7-256
7. Yousry TA, Pelletier D, Cadavid D, et al. Magnetic resonance imaging pattern in natalizumab-associated progressive multifocal leukoencephalopathy. *Ann Neurol*. 2012;72(5):779-787. https://doi.org/10.1002/ana.23676
8. Hodel J, Darchis C, Outteryck O, et al. Punctate pattern: a promising imaging marker for the diagnosis of natalizumab-associated PML. *Neurology*. 2016;86(16):1516-1523.
9. Wijburg MT, Witte BI, Vennegoor A, et al. MRI criteria differentiating asymptomatic PML from new MS lesions during natalizumab pharmacovigilance. *J Neurol Neurosurg Psychiatry*. 2016;87(10):1138-1145. https://doi.org/10.1136/jnnp-2016-313772
10. Wattjes MP, Wijburg MT, Vennegoor A, et al. MRI characteristics of early PML-IRIS after natalizumab treatment in patients with MS. *J Neurol Neurosurg Psychiatry*. 2016;87(8):879-884. https://doi.org/10.1136/jnnp-2015-311411
11. Wattjes MP, Wijburg MT, van Eijk J, et al. Inflammatory natalizumab-associated PML: baseline characteristics, lesion evolution and relation with PML-IRIS. *J Neurol Neurosurg Psychiatry*. 2018;89(5):535-541. https://doi.org/10.1136/jnnp-2017-316886
12. Clifford DB, DeLuca A, Simpson DM, Arendt G, Giovannoni G, Nath A. Natalizumab-associated progressive multifocal leukoencephalopathy in patients with multiple sclerosis: lessons from 28 cases. *Lancet Neurol*. 2010;9(4):438-446. https://doi.org/10.1016/S1474-4422(10)70028-4
13. Riedel DJ, Pardo CA, McArthur J, Nath A. Therapy insight: CNS manifestations of HIV-associated immune reconstitution inflammatory syndrome. *Nat Clin Pract Neurol*. 2006;2(10):557-565. https://doi.org/10.1038/ncpneuro0303
14. Epperla N, Medina-Flores R, Mazza JJ, Yale SH. Mirtazapine and mefloquine therapy for non-AIDS-related progressive multifocal leukoencephalopathy. *Wis Med J*. 2014;113(6):242-245.
15. Marshall LJ, Major EO. Molecular regulation of JC virus tropism: insights into potential therapeutic targets for progressive multifocal leukoencephalopathy. *J Neuroimmune Pharmacol*. 2010;5(3):404-417. https://doi.org/10.1007/s11481-010-9203-1
16. Clifford DB, Yiannoutsos C, Glicksman M, et al. HAART improves prognosis in HIV-associated progressive multifocal leukoencephalopathy. *Neurology*. 1999;52(3):623-625. https://doi.org/10.1212/wnl.52.3.623
17. Cortese I, Muranski P, Enose-Akahata Y, et al. Pembrolizumab treatment for progressive multifocal leukoencephalopathy. *N Engl J Med*. 2019;380(17):1597-1605. https://doi.org/10.1056/NEJMoa1815039
18. Stork L, Brück W, Bar-Or A, Metz I. High CCR5 expression in natalizumab-associated progressive multifocal leukoencephalopathy immune reconstitution inflammatory syndrome supports treatment with the CCR5 inhibitor maraviroc. *Acta Neuropathol*. 2015;129(3):467-468. https://doi.org/10.1007/s00401-015-1391-6
19. Berger JR, Aksamit AJ, Clifford DB, et al. PML diagnostic criteria: consensus statement from the AAN neuroinfectious disease section. *Neurology*. 2013;80(15):1430-1438. https://doi.org/10.1212/WNL.0b013e31828c2fa1
20. Bossolasco S, Calori G, Moretti F, et al. Prognostic significance of JC virus DNA levels in cerebrospinal fluid of patients with HIV-associated progressive multifocal leukoencephalopathy. *Clin Infect Dis*. 2005;40(5):738-744. https://doi.org/10.1086/427698
21. Živanović M, Savšek L, Poljak M, Popović M. Possible pitfalls in the diagnostic of progressive multifocal leukoencephalopathy. *Clin Neuropathol*. 2016;35(2):66-71. https://doi.org/10.5414/NP300911
22. Khoury MN, Alsop DC, Agnihotri SP, et al. Hyperintense cortical signal on magnetic resonance imaging reflects focal leukocortical encephalitis and seizure risk in progressive multifocal leukoencephalopathy. *Ann Neurol*. 2014;75(5):659-669. https://doi.org/10.1002/ana.24144
23. Aly L, Yousef S, Schippling S, et al. Central role of JC virus-specific CD4+ lymphocytes in progressive multi-focal leucoencephalopathy-immune reconstitution inflammatory syndrome. *Brain*. 2011;134(Pt 9):2687-2702. https://doi.org/10.1093/brain/awr206
24. Metz I, Radue EW, Oterino A, et al. Pathology of immune reconstitution inflammatory syndrome in multiple sclerosis with natalizumab-associated progressive multifocal leukoencephalopathy. *Acta Neuropathol*. 2012;123(2):235-245. https://doi.org/10.1007/s00401-011-0900-5
25. Haller S, Kövari E, Herrmann FR, et al. Do brain T2/FLAIR white matter hyperintensities correspond to myelin loss in normal aging? A radiologic-neuropathologic correlation study. Published online 2013. http://www.actaneurocomms.org/content/1/1/14. Accessed August 26, 2021.
26. Bitsch A, Kuhlmann T, Stadelmann C, Lassmann H, Lucchinetti C, Brück W. A longitudinal MRI study of histopathologically defined hypointense multiple sclerosis lesions. *Ann Neurol*. 2001;49(6):793-796.
27. Sahraian MA, Radue EW, Eshaghi A, Besliu S, Minagar A. Progressive multifocal leukoencephalopathy: a review of the neuroimaging features and differential diagnosis. *Eur J Neurol*. 2012;19(8):1060-1069. https://doi.org/10.1111/j.1468-1331.2011.03597.x
28. Shah R, Bag AK, Chapman PR, Curé JK. Imaging manifestations of progressive multifocal leukoencephalopathy. *Clin Radiol*. 2010;65(6):431-439. https://doi.org/10.1016/j.crad.2010.03.001
29. Zeiner PS, Preusse C, Blank A-E, et al. MIF receptor CD74 is restricted to microglia/macrophages, associated with a M1-polarized immune milieu and prolonged patient survival in gliomas. *Brain Pathol*. 2015;25(4):491-504. https://doi.org/10.1111/bpa.12194
30. Gray F, Bazille C, Adle-Biassette H, Mikol J, Moulignier A, Scaravilli F. Central nervous system immune reconstitution disease in acquired immunodeficiency syndrome patients receiving highly active antiretroviral treatment. *Journal of NeuroVirology*. 2005;11(SUPPL. 3):16-22. https://doi.org/10.1080/13550280500511741
31. Vendrely A, Bienvenu B, Gasnault J, Thiebault JB, Salmon D, Gray F. Fulminant inflammatory leukoencephalopathy associated with HAART-induced immune restoration in AIDS-related progressive multifocal leukoencephalopathy. *Acta Neuropathol*. 2005;109(4):449-455. https://doi.org/10.1007/s00401-005-0983-y
32. Martin-Blondel G, Bauer J, Cuvinciuc V, et al. In situ evidence of JC virus control by CD8+ T cells in PML-IRIS during HIV infection. *Neurology*. 2013;81(11):964-970. https://doi.org/10.1212/WNL.0b013e3182a43e6d
33. Fournier A, Martin-Blondel G, Lechapt-Zalcman E, et al. Immune reconstitution inflammatory syndrome unmasking or worsening AIDS-related progressive multifocal leukoencephalopathy: a literature review. *Front Immunol*. 2017;8:577. https://doi.org/10.3389/fimmu.2017.00577
34. Tan K, Roda R, Ostrow L, McArthur J, Nath A. PML-IRIS in patients with HIV infection: clinical manifestations and treatment with steroids. *Neurology*. 2009;72(17):1458-1464. https://doi.org/10.1212/01.wnl.0000343510.08643.74
35. Weber T, Trebst C, Frye S, et al. Analysis of the systemic and intrathecal humoral immune response in progressive multifocal

leukoencephalopathy. *J Infect Dis*. 1997;176(1):250-295. https://doi.org/10.1086/514032
36. Du Pasquier RA, Kuroda MJ, Zheng Y, Jean-Jacques J, Letvin NL, Koralnik IJ. A prospective study demonstrates an association between JC virus-specific cytotoxic T lymphocytes and the early control of progressive multifocal leukoencephalopathy. *Brain*. 2004;127(Pt 9):1970-1978. https://doi.org/10.1093/brain/awh215
37. Wüthrich C, Kesari S, Kim W-K, et al. Characterization of lymphocytic infiltrates in progressive multifocal leukoencephalopathy: co-localization of CD8(+) T cells with JCV-infected glial cells. *J Neurovirol*. 2006;12(2):116-128. https://doi.org/10.1080/13550280600716604
38. Moll NM, Rietsch AM, Ransohoff AJ, et al. Cortical demyelination in PML and MS: similarities and differences. *Neurology*. 2008;70(5):336-343. https://doi.org/10.1212/01.WNL.0000284601.54436.e4
39. Leng L, Metz CN, Fang Y, et al. MIF signal transduction initiated by binding to CD74. *J Exp Med*. 2003;197(11):1467-1476. https://doi.org/10.1084/jem.20030286
40. Zeiner PS, Preusse C, Golebiewska A, et al. Distribution and prognostic impact of microglia/macrophage subpopulations in gliomas. *Brain Pathol*. 2019;29(4):513-529. https://doi.org/10.1111/bpa.12690

SUPPORTING INFORMATION

Additional supporting information may be found in the online version of the article at the publisher's website.

How to cite this article: Zeiner PS, Mann L, Filipski K, et al. Immune profile and radiological characteristics of progressive multifocal leukoencephalopathy. *Eur J Neurol*. 2022;29:543–554. https://doi.org/10.1111/ene.15140